European Water 32: 35-45, 2010.

Embankment Dam Failure: A Downstream Flood Hazard Assessment

G. Tsakiris[1], V. Bellos[2] and C. Ziogas[3]
[1] *National Technical University of Athens, School of Rural and Surveying Engineering, Centre for the Assessment of Natural Hazards and Proactive Planning and Laboratory of Reclamation Works and Water Resources Management, 9 Iroon Polytechniou, 15780, Athens – Greece, e-mail: water@survey.ntua.gr*
[2] *National Technical University of Athens, Postgraduate Course "Water Resources: Science and Technology", 9 Iroon Polytechniou, 15780, Athens – Greece,e-mail: ps10019@mail.ntua.gr*
[3] *Democritus University of Thrace, Department of Civil Engineering, Ph.d Student, 12 Vas. Sofias, 67100, Xanthi –Greece, e-mail:kostaschziogas@gmail.com*

Abstract: The flood hazard assessment in the downstream valley from a possible dam failure requires a comprehensive modelling of the breach formation, the outflow through the breach, and the routing of flood wave in the downstream valley. Several analytical and numerical methods have been proposed to simulate the entire process the most popular of which are those proposed by the Nat. Weather Service of USA. This paper presents an application of the above tools in a risk assessment study of a new embankment dam which is under construction in Crete (Greece). The hydrograph at selected cross-sections of the valley downstream the dam and the inundation area from the hypothetical dam failure were determined for three failure times. It was shown that the results are quite sensitive in relation to the time of failure adopted. Furthermore, other parameters influencing the peak outflow and the inundation area are explained and discussed.

Key words: Flood hazard, embankment dam, dam failure, inundation area, floodwave routing, breach formation

1. INTRODUCTION

The construction of dams serves a number of purposes such as water supply, irrigation, hydroelectric power generation, and flood control. In many cases flood control constitutes a secondary function of the dam operation since apart from its main operation, its storage contributes to the attenuation of flood peaks. However although the existence of a dam contributes to the flood prevention in the downstream area, ironically, it may cause an even more severe flood downstream in case of its failure.

Dams constructed in recent years may be classified into two broad categories dependent upon the construction material: the rigid dams (concrete gravity, RCC etc.) and the flexible dams (earthfill, rockfill etc.). The main feature of flexible dams is that they are built with a central impervious core sandwiched by filter material for coverage and stability of the core. The principal advantages of the flexible dams over the rigid ones are: a) the use of locally available natural materials requiring minimum processing and b) the tolerance against micro-movements of the dam foundation. However, flexible dams demonstrate also two significant disadvantages: a) the material erosibility under the erosive action of overtopping water (thus an increased probability of failure due to overtopping) and b) the increased probability of failure due to “piping”.

Worldwide some hundreds of dams have failed creating catastrophic consequences and significant number of deaths. In the literature there exist Databases containing a significant number of dam failures accompanied by the most basic parameters of these dam failures. However most of these Databases contain either wrong data or incomplete data. Recently, the Centre for the Assessment of Natural Hazards and Proactive Planning of the National Technical University of Athens compiled two tables containing the most severe dam breaks worldwide, one for large dams and one for small dams (height less than 30 m). The table for large dam failures is reproduced in Table 1 of this article.

Using historical dam failures several researchers have derived important conclusions on the range of the basic parameters of dam failure such as the time of breach formation, the average width of the breach and the peak outflow from the breach. (e.g. Froehlich, 1995 and 2008, Walder and O´Connor, 1997, Wahl, 2004). Recently Tsakiris and Spiliotis (2010) assisted by the data of Table 1, formulated a semi-analytical method for simulating the breach formation process of an embankment dam failure and the development of outflow hydrograph based on the parabolic shape of the breach.

Table 1. List of large dam failures (Source: CANAH, 2010)

No	Dam name	Country	Year completed	Year failed	Failure mode	Height of dam	Storage	Peak outflow	Height of water above breach bottom of failure	Breach shape	Height of breach	Top breach width	Bottom breach width	Average breach width	Breach formation time
						m	$x10^6$ m^3	$x10^3$ m^3/s	m		m	m	m	m	h
1	Alcova, Wyoming	USA	1938	1968		81.0	227.0								
2	Apishapa, Colorado	USA	1920	1923	Piping	34.1	22.5	6.85	28.0	trapezoid	31.1	91.5	81.5	93.0	0.75
3	Baldwin Hills, Calif.	USA	1951	1963	Piping	71.0	1.1	1.13	12.2	triangular	21.3			25.0	0.33
4	Belden, Calif.	USA	1958	1967		50.0	3.0								
5	Bradfield	UK	1863	1864	Piping	29.0	3.2	1.15							
6	Cheney, Kansas	USA	1965	1971		38.0	306.0								
7	Dantiwada	India	1965	1973		41.6	464.0	7.50							
8	Euclides de Cunha	Brazil	1958	1977	Overtopping	53.0	13.6	1.02	58.2	trapezoid	53.0	131.0			
9	Hell Hole, Calif.	USA	1964	1964	Piping	67.0	30.6	7.36	35.1	trapezoid	56.4			121.0	0.75
10	Khadkawasla	India	1879	1961		31.0	2.8	2.78							
11	Lower Otay, Calif.	USA	1897	1916	Overtopping	41.2	49.3		39.6	trapezoid	39.6	172.2	93.8	133.0	1.00
12	Machhu II	India	1972	1979	Seepage	60.0	110.0				60.0	540.0			
13	Malpasset	France	1954	1959		66.5	51.0								
14	Oros	Brazil	1960	1960	Overtopping	35.4	650.0	9.63	35.8	trapezoid	35.5	200.0	130.0	165.0	8.50
15	Salles Oliveira	Brazil	1966	1977	Overtopping	35.0	25.9	7.20	38.4	trapezoid	35.0			168.0	
16	Schaeffer, Colorado	USA	1909	1921	Overtopping	30.5	3.9	4.50	30.5	trapezoid	30.5	210.0	64.0	137.0	0.50
17	Sherman, Nebraska	USA	1959	1962		41.0	85.2								
18	St. Francis, Calif.	USA	1926	1928		62.5	46.9	14.1							
19	Swift, Montana	USA	1914	1964	Overtopping	57.6	37.0	24.9	47.8	trapezoid	57.6	225.0	225.0	225.0	
20	Teton, Idaho	USA	1975	1976	Piping	93.0	356.0	65.12	77.4	trapezoid	86.9			151.0	1.25
21	Vaiont	Italy	1959	1963	Overtopping	267.0	240.0								
22	Walter Bouldin, Alab.	USA	1967	1975	Seepage	50.0									

In this paper an interesting application of the entire dam failure process, the development of the outflow hydrograph and the routing of floodwave through the downstream valley is presented. The principal method used is the FLDWAV model proposed by the National Weather Service of USA (Fread et al., 1993). As will be seen interesting conclusions were obtained related to the sensitivity of the results against the most critical determinant which is the time of failure.

2. DAM BREAK STATISTICS

Interesting statistical studies on the historical dam failures had as a result the estimation of the dam failure determinants from regression equations. Namely the most important quantity the peak outflow was proposed to be estimated by the following regression equation (Froehlich, 1995):

$$Q_{\max} = 0.607 V_w^{0.295} H_w^{1.24} \tag{1}$$

where Q_{max} is the predicted peak outflow (m^3/s); V_w is the volume of water in the reservoir at the time of failure (m^3) and H_w is the depth of water in the reservoir at the time of failure above the final

bottom level of the breach (m). It is supported that the failure mode and the average embankment width does not improve the regression equation significantly.

Further Froehlich (2008) based on the same data base proposed the following equations for the estimation of the breach formation time t_f (h) and the mean breach width $\overline{B}$ (m):

$$t_f = 63.2\sqrt{\frac{V_w}{gH_b^2}} \tag{2}$$

$$\overline{B} = 0.27k_0V_w^{1/3} \tag{3}$$

where H_b is the height of the breach (m) and k_0 constant (1.3 for overtopping failures and 1.0 for other failure modes).

Concerning the breach side slope of the trapezoidal shape of the breach 1:m (v:h) Froehlich (2008) proposed m to be taken as 1.0 for overtopping failure and 0.7 for other failure modes.

A simple empirical formula for reservoirs of less than 10 million m^3 (proposed by Lemperier, 1995) yields the order of magnitude for flood peak Q_{max} (m^3/s) versus headwater depth h_d (m) at the breach and reservoir storage V_w (m^3 x 10^3) at the time of failure:

$$Q_{\max} = KH_b^{1.5}V^{0.5} \tag{4}$$

where K varies from 10 (well-compacted clay) and 25 (fill without cohesion).

3. DAM BREAK AND FLOOD WAVE PROPAGATION

The hydraulic process of the dam break incident and the subsequent flood wave propagation in a natural channel have attracted the attention of many researchers in the past. From the three processes (breach formation, outflow hydrograph development and routing of flood wave downstream the dam), the latter can be described by the well known equations of Saint-Venant. These equations comprise an equation of mass conservation and an equation of momentum conservation. These equations, in their conservative form (with additional coefficients for the effect of the river contraction and expansion) can be written:

$$\frac{\partial Q}{\partial x} + \frac{\partial\left(A + A_0\right)}{\partial t} - q = 0 \tag{5}$$

$$\frac{\partial Q}{\partial t} + \frac{\partial\left(\beta Q^2 / A\right)}{\partial x} + gA\left(\frac{\partial h}{\partial t} + S_f\right) = 0 \tag{6}$$

where Q is the flow; h is the water surface elevation; A is the wetted active cross-sectional area; A_0 is the wetted inactive off-channel (dead) storage area; x is the distance measured along the mean flow path; t is the time; q is the lateral flow (inflow is positive and outflow is negative); β is the coefficient of momentum for velocity allocation; g is the gravity acceleration constant; S_f is the friction slope; and B is the wetted top width of flow cross section at elevation h.

The friction slope S_f in Eq. (6) is customarily determined by the Manning formula assuming steady flow conditions:

$$S_f = \frac{n^2|Q|Q}{A^2 R^{4/3}} = \frac{|Q|Q}{K^2} \tag{7}$$

in which R is the hydraulic radius and K is the total conveyance.

The expanded equations of Saint–Venant (Eqs (5) and (6)) constitute a scheme of non-linear, differential equations with two independent variables, x and t, and two dependent ones, h and Q. These equations cannot be solved analytically except for the case that the channel geometry and the boundary conditions are simple so that the nonlinear components of the equations can be ignored or transformed into linear ones. Eqs (5) and (6) can be solved numerically by implementing the following two steps. Firstly, the differential equations are represented by a corresponding set of algebraic finite difference equations. Secondly, this set is solved taking into account the initial and boundary conditions.

The literature contains numerous models on flood routing, the majority of which are general purpose models that have not been designed specifically to deal with the extreme conditions that characterize a dam failure. In this study, the well known software package FLDWAV, developed by the NWS (National Weather Service of USA) has been used. FLDWAV model constitutes a general flood propagation model that is based on a solution of finite differences of the complete Saint – Venant equations and on the implicit numerical scheme of Preissman (Fread, 1984a 1984b, Fread et al., 1993).

This model is based on a weighted four-point nonlinear implicit finite difference numerical technique that was first implemented by Preissmann (1961). It exhibits several advantages since it can be implemented at uneven intervals of time and space.

In this technique, the continuous interval of space and time (x – t), in which the solutions of the variables h and Q will be derived, is represented by a rectangular network of discrete points. The time derivatives are estimated by the quotient of a front difference between the points i and i+1 along the x axis, i.e.:

$$\frac{\partial \Psi}{\partial t} = \frac{\Psi_i^{j+1} + \Psi_{i+1}^{j+1} - \Psi_i^j - \Psi_{i+1}^j}{2\Delta t_j} \tag{8}$$

The space derivatives are approximately estimated by the quotient of a front difference between two adjacent time elements, according to the weighted components of θ and (1-θ), i.e.:

$$\frac{\partial \Psi}{\partial t} = \theta\left[\frac{\Psi_{i+1}^{j+1} - \Psi_i^{j+1}}{\Delta x_i}\right] + (1-\theta)\left[\frac{\Psi_{i+1}^j - \Psi_i^j}{\Delta x_i}\right] \tag{9}$$

Except from the derivatives, other variables are approximated in terms of time whereas the space derivatives are estimated by the same weighted components, i.e.:

$$\Psi = \theta\left[\frac{\Psi_i^{j+1} - \Psi_{i+1}^{j+1}}{2}\right] + (1-\theta)\left[\frac{\Psi_i^j - \Psi_{i+1}^j}{2}\right] \tag{10}$$

The equations that are derived from the discretisation of Eqs (5) and (6) can not be solved with an explicit method since they include four unknown variables Q_i^{j+1}, h_i^{j+1}, Q_{i+1}^{j+1}, h_{i+1}^{j+1} with only two equations. Nevertheless, if Eqs (5) and (6) are applied for each of the (N-1) rectangular grids between the upstream and downstream boundaries, then a set of (2N-2) equations with 2N unknown variables is derived. The boundary conditions of the subcritical flow give the additional two equations required for the scheme solution. The derived scheme of the 2N unknown variables and

the 2N nonlinear equations can be solved via an iterative procedure, the Newton-Raphson technique. The upstream and downstream boundary conditions are also determined.

As far as the upstream boundary conditions are concerned, it is well known that embankment dams do not fail instantaneously or completely. The fully formed breach in earthen large dams tends to be estimated with an average width $\overline{B}$ at the range $0.5h_d \le \overline{B} \le 8.0h_d$, where h_d is the height of the dam. In a recent study Tsakiris and Spiliotis (2010) using the list of Dam breaks of the Centre for the Assessment of Natural Hazards and Proactive Planning (Nat. Technical University of Athens) (Table 1) estimated the range of the ratio $\overline{B}/h_d$ between 2.0 and 5.5. Breach width of earthen dams is therefore expected to be much smaller than the total length of the dam. Also, the final breach formation requires a certain period of time dependent on the construction material, the cause of failure, the height of the dam and a number of other factors characterizing the dam, the reservoir, and the initial conditions. For the most common cause which is the overtopping, the time of failure may range from few minutes to one or two hours. According to Tsakiris and Spiliotis (2010) the key determinant is not the time of failure itself but the rate of vertical erosion which was estimated to vary between 10 and 130 m/h.

It is very important to note that the outflow hydrograph and the peak outflow are governed largely by the rate of breach formation which practically is equal to vertical erosion rate.

Several models of varying complexity were developed in the past with the aim to simulate the failure process (e.g. Cristofano, 1965, Ponce and Tsivoglou, 1981, Wurbs, 1987, Singh and Quiroga, 1987 a, b). These models assumed that the dam failure process develops gradually and that the breach is generally of a trapezoidal shape and in rare cases of a rectangular or triangular shape.

According to Fread (1988) the outflow hydrograph can be calculated by the following equation:

$$Q_b = c_v k_s \left[3.1 b_i (h - h_b)^{1.5} + 2.45 m (h - h_b)^{2.5}\right] \tag{11}$$

in which Q_b is the discharge; c_v is a small computed correction for the velocity; b_i is the computed instantaneous breach bottom; h is the computed elevation of the water surface just upstream of the dam; h_b is the computed elevation of the breach bottom which is assumed to be a function of the breach formation time t_f. The symbol m is the side slope of the breach and k_s is the computed submergence correction due to the downstream tailwater elevation h_t.

The above mentioned parameters can be calculated by the following equations:

$$b_i = b\left(\frac{t}{t_f}\right)^{\rho} \quad \text{if} \quad 0 < t \le t_f \tag{12}$$

$$h_b = h_d - (h_d - h_{bm})\left(\frac{t}{t_f}\right)^{\rho} \tag{13}$$

in which h_{bm} is the final elevation of the breach bottom which is usually, but not necessarily, the bottom of reservoir or outlet channel bottom; t is the time since beginning of breach formation and ρ is the parameter specifying the degree of nonlinearity ($1 \le \rho \le 4$).

$$k_s = 1.0 - 27.8\left(\frac{h_t - h_b}{h - h_b} - 0.67\right)^3 \quad \text{if} \quad \frac{h_t - h_b}{h - h_b} \ge 0.67 \tag{14}$$

otherwise $k_s = 1.0$.

3. CASE STUDY

The following case study was performed for the analysis of the consequences of a hypothetical failure of the Aposelemis dam which is under construction in Crete, Greece (Fig.1)

The entire area of Aposelemis river watershed is 120 km^2 and at the dam site the watershed size is 62 km^2. As can be seen in Fig.1 there is an interconnection between the Aposelemis river watershed and the Lasithi plateau. The effect of this connection however is not considered in the computation of breach formation and flood wave propagation. Since the dam site is located only 14 km from the mouth of the river to the sea any dam failure will result in immediate consequences in the coastal zone of the watershed.

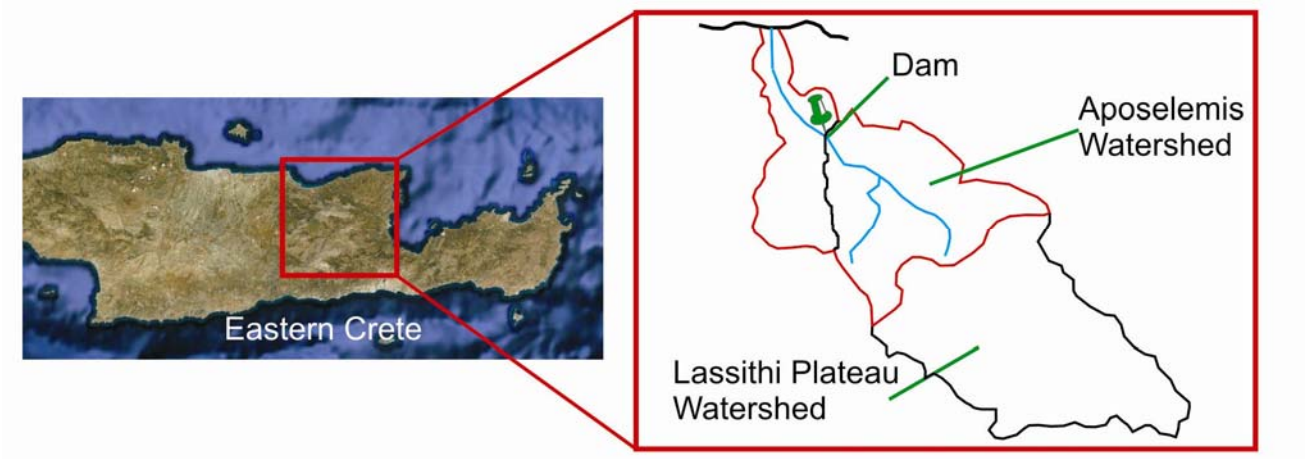

Figure 1. The watershed of the study area

The data used are based to a) on the technical and feasibility studies for the dam construction, b) the stage - surface area and stage - volume functions of the reservoir and c) the maps of the area of the reservoir and the watershed.

The dam is an earthen embankment dam with an impervious clay core. The crest length is 650 m, the crest elevation is 222.0 m asl, and the height of the dam above the initial river bed is 52 m. According to the technical report the spillway of the dam is 40 m and its crest elevation is 216.5 m asl. The reservoir capacity was estimated 40 x 10^6 m^3.

As mentioned above the FLDWAV model was used for the simulation of the dam break and the flood wave propagation.

Several assumptions related to the failure process were adopted. For instance the final breach dimensions were produced by the bottom width of the breach equal to 40 m, and the elevation of the breach bottom at 170 m asl. The breach was assumed trapezoidal with side slopes 1:1.5 (vertical/horizontal) (Fig.2).

Such assumptions produce rather conservative estimations with respect to peak outflow and the inundated area downstream in case of a dam failure incident. If Eqs (2) and (3) were to be applied then t_f=0.75 h and $\overline{B}$=139 m.

The outflow hydrograph has been calculated using different times for the breach formation: t_f=2.5, 1.0 and 0.25 h. The calculated flow hydrographs are shown in Figs (3), (4) and (5) and the stage hydrographs in Figs (6), (7) and (8) for three selected locations a) downstream close to the dam, b) at a distance 1.34 km downstream the dam where the village Potamies is located and c) at a distance 5.15 km downstream the dam. It is very remarkable to notice that the results are very sensitive to the time of failure and more precisely to the rate of vertical erosion. At the cross-section close to the dam the outflow hydrograph is in fact the outflow hydrograph from the breach. In gross terms the peak outflow varies from 10000 to 29000 m^3/s (for t_f 2.5 h and 0.25 h, respectively). For t_f 1 h the peak outflow from the breach is estimated as 20000 m^3/s approximately). This shows that no single estimation is sufficient and that at least two boundary values for the time of failure are

always needed to accompany the medium "most probable" time of failure in case the designer seeks a better understanding of the dam break process and the potential consequences in the area downstream the dam.

An interesting point is also the rate of decline of peak flow as we move to cross sections at considerable distances from the dam. Considering the results for t_f=1 h we can observe a rather gentle decline of the peak flow as we move downstream. The peak outflow from 20000 m^3/s near the dam becomes 16000 m^3/s at the cross-section 5.15 km downstream the dam. This is explained mainly by the morphology of the valley downstream the dam which remains narrow even after this distance downstream.

Also, in Figs (9) and (10) the longitudinal profile of the peak flow and the longitudinal profile of the maximum water levels are shown respectively. In particular Fig.10 can be used for estimating the depth of water which may be reached in case of the dam break. It is of great interest to notice that in the village of Potamies with 700 people which is located 1.34 km downstream the dam, a possible dam break can cause waves with more than 10 m depth.

It seems that even under the most favourable conditions for the dam failure (due to the assumption adopted) the community of Potamies, will be flooded within few minutes (according to the second scenario with time of failure t_f=1 h, Fig.4). The potential consequences in the coastal zone however will be assessed from the detailed analysis of flood wave propagation under the most unfavourable conditions, t_f=0.25 h (Figs 9 and 10).

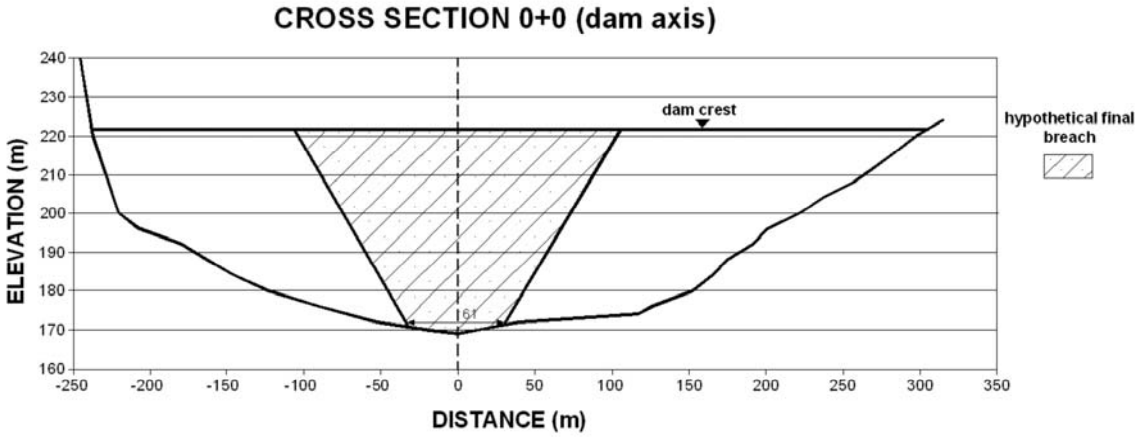

Figure 2. Cross – section of the dam and dam breach

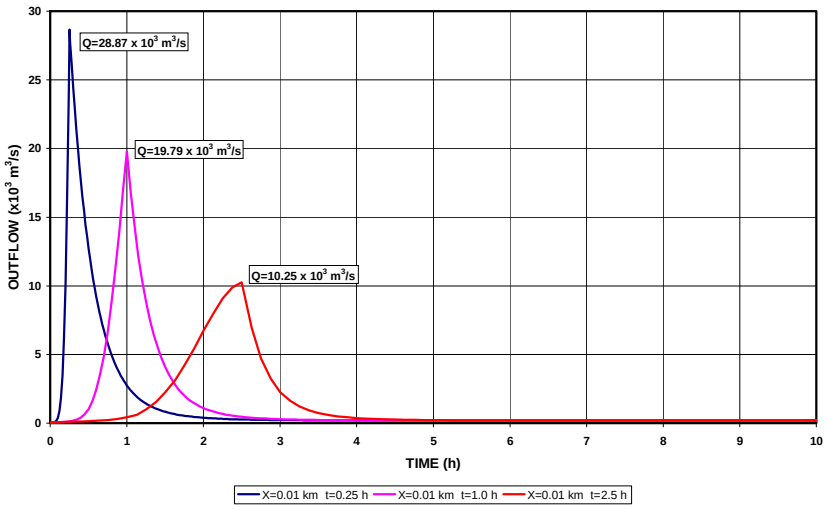

Figure 3. Flow Hydrographs at the position 0 + 010 m

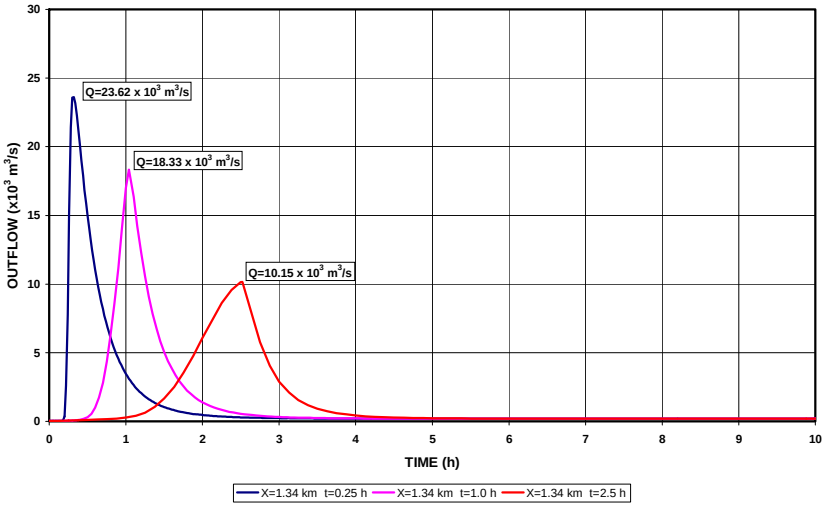

Figure 4. Flow Hydrographs at the position 1 + 340 m

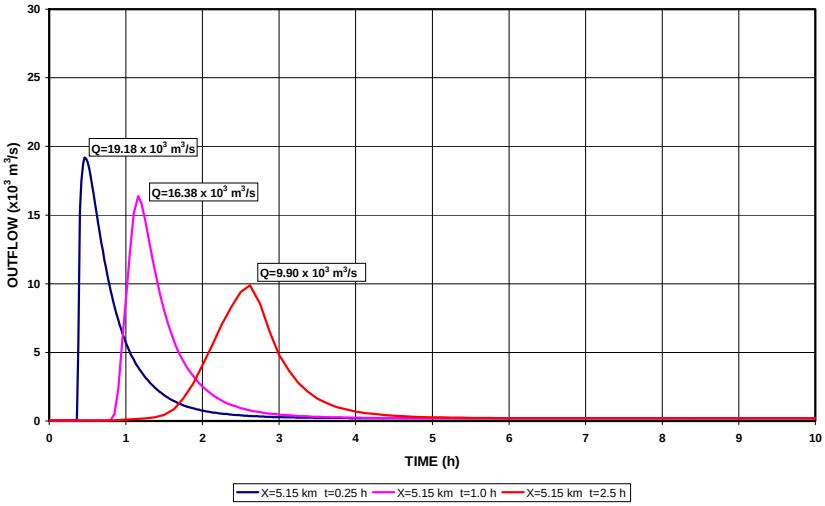

Figure 5. Flow Hydrographs at the position 5 + 150 m

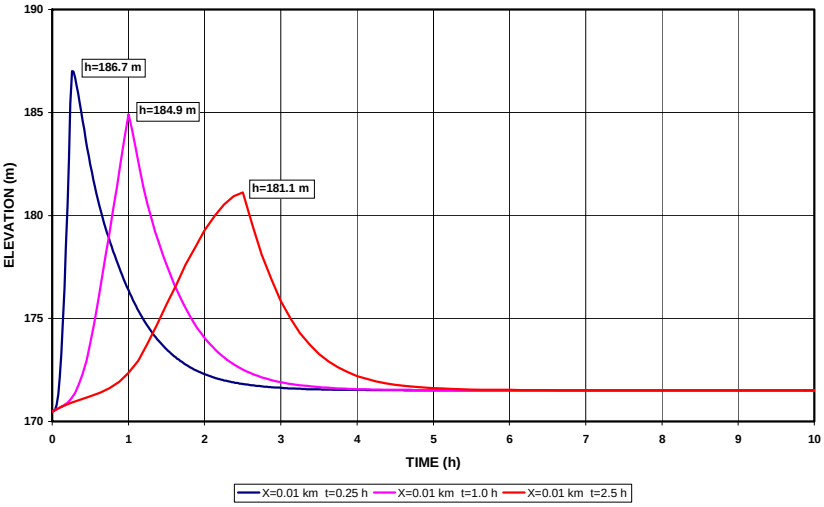

Figure 6. Stage Hydrographs at the position 0 + 010 m

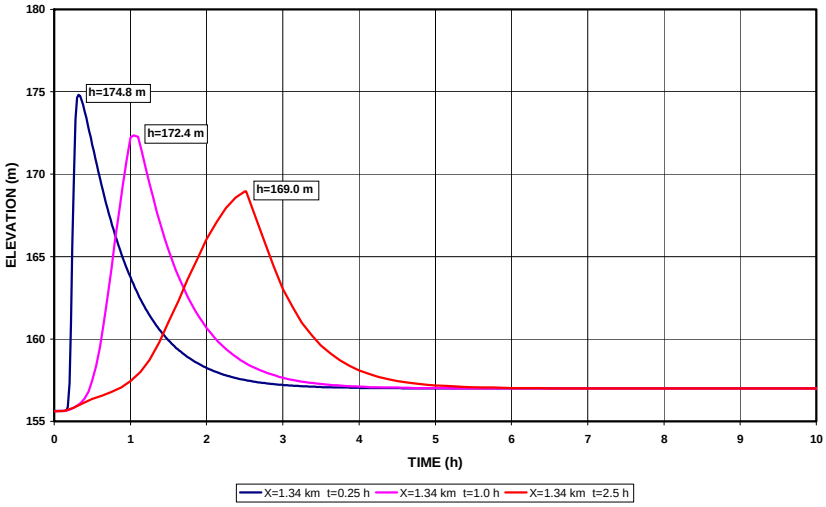

Figure 7. Stage Hydrographs at the position 1 + 340 m

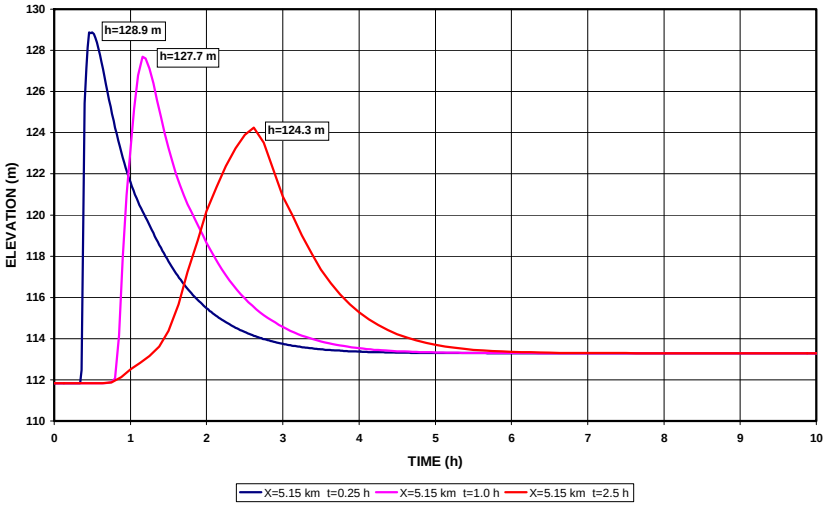

Figure 8. Stage Hydrographs at the position 5 + 150 m

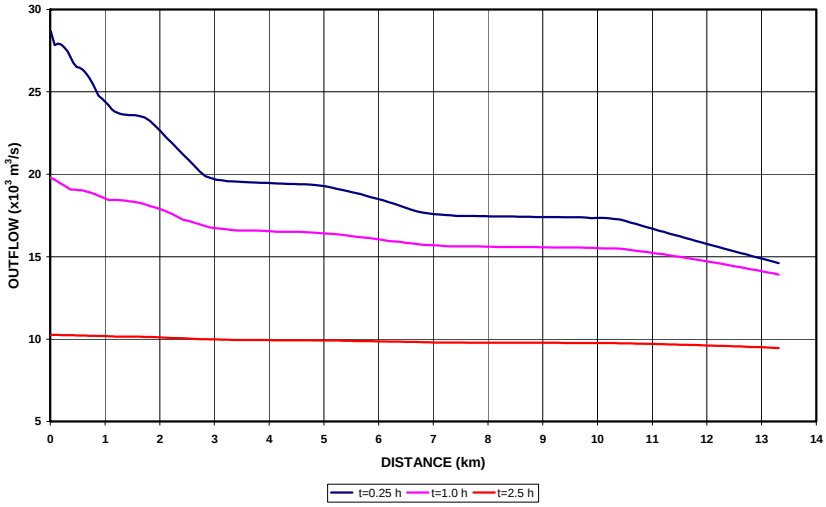

Figure 9. Longitudinal profile of max discharges

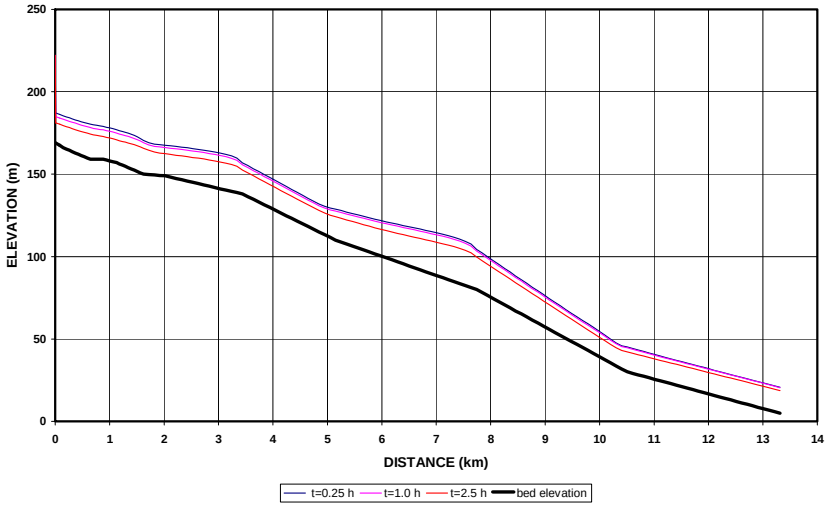

Figure 10. Longitudinal profile of max water levels

Finally the potentially inundated area downstream in case of the dam failure is presented in Fig. (11a, b, c) corresponding to the three scenaria examined. In these figures most of the village of Potamies seems to be inundated in case of such incident.

Figure 11. The inundation area for the three times of failure (a: tf=2.5h, b: tf=1h, c: tf=0.25h)

4. CONCLUSIONS

An interesting application of an embankment dam break was presented in the framework of a risk assessment study related to the construction of a new dam in the island of Crete. The dam breach formation, the outflow hydrograph development and the inuntation area estimation were produced using the FLDWAV model for three times of failure 2.5 ,1 and 0.25 h which correspond to vertical erosion of 21, 52 and 208 m/h respectively. As expected, the time of failure influences considerably the peak outflow from the breach and the inuntated area caused by the dam break.

It was concluded that for such a study the most probable vertical erosion rate together with an upper and a lower rate gives the designer a comprehensive understanding of the dam break consequences.

Since the time of failure (or the rate of vertical erosion) is the most variable parameter it may be studied by representing it as a fuzzy number and applying fuzzy set theory for calculating peak outflow and the potentially inundated area downstream the dam.

REFERENCES

CANAH, 2010. List of large dam failures. http://naturalhazards.ntua.gr/.

Cristofano, E. A., 1965. Method of computing erosion rate for failure of earthfill dams. United States Bureau of Reclamation, Denver, Colorado.

Fread, D. L., 1984a. A breach erosion model for earthen dams. Hydrologic Research Laboratory, National Weather Service, Silver Spring, Maryland.

Fread, D. L., 1984b. DMBRK: The NWS dam-break flood forecasting model. Office of Hydrology, National Weather Service, Silver Spring, Maryland.

Fread, D. L., and Lewis, J. M., 1988. FLDWAV: A generalizated flood routing model. Proceedings of National Conference on Hydraulic Engineering, Colorado Springs, Colorado.

Fread, D. L., and Lewis, J.M., 1993. NWS FLDWAV Model: The replacement of DAMBRK for dam break flood prediction. Proc. 10th Annual Conference of the Association of State Dam Safety Officials, Inc., Kansas City, Missouri, pp. 177-184.

Froehlich, D. C., 1995. Peak Outflow from breached embankment dam. Journal of Water Resources Planning Mannagement, ASCE, 134(12): 1708-1721.

Froehlich, D., 2008. Embankment Dam Breach Parameters and Their Uncertainties. Journal of Hydraulic Engineering, ASCE, 121(1): 90-97.

Lemperier, F. (1995). “Dam cost and safety, Water and Energy 2001, International R&D Conference, New Delhi, India.

Ponce, V. M., and Tsivoglou, A. J., 1981. Modeling of gradual dam breaches. Journal of Hydraulic Division, ASCE, 107, HY6, June, pp. 829-838.

Preissmann, A., 1961. Propagation des intoumescences dans les canaux et reviers, First Congress of the French Ass. for Computation, Grenoble, Sept. 14-16. Procc., A.F.C.A.L., 433-442.

Singh, V., and Quiroga, C. (1987a). “A dam breach erosion model: I. Formulation, Water Resources Management, Vol I(3), pp. 177-197.

Singh, V., and Quiroga, C. (1987b). “A dam breach erosion model: II. Application, Water Resources Management, Vol I(3), pp. 199-221.

Tsakiris, G., and Spiliotis, M., 2010. Dam-breach hydrograph modelling: An innovative semi-analytical approach. Paper to be presented in the 6th International Symposium of EWRA, Catania, June 29-July 2, 2011 (under review)

Wahl, T. L., 2004. Uncertainty of predictions of embankment dam breach parameters. Journal of hydraulic engineering. ASCE, 130(5): 389-397.

Walder, J. S., and O' Connor, J. E., 1997. Methods for predicting peak discharge of floods caused by failure of natural and constructed earth dams. Water Resource Research, 33(10): 2337-2348.

Wurbs, R. 1987. Dam-breach wave models. Journal of Hydraulic Engineering, ASCE, Vo. 113, No 1, January, pp. 29-46.